November 1996 *Chem. Pharm. Bull.* **44**(11) 1989—1997 (1996) 1989

Relationship between X- or L-Band ESR Spectra and Coordination Structures of Copper(II) Complexes with a CuO_4 Coordination Mode[1]

Katsuya FUKUMARU, Takashi SAWADA, Norihisa NISHINO, and Hiromu SAKURAI*

Department of Analytical and Bioinorganic Chemistry, Kyoto Pharmaceutical University, Nakauchi-cho 5, Misasagi, Yamashina-ku, Kyoto 607, Japan. Received May 22, 1996; accepted July 19, 1996

ESR spectrometry is useful for studying the coordination environment around lone pair electrons of paramagnetic metal ions, such as the copper(II) (Cu(II)) ion. To this purpose, X-band ESR spectrometry has generally been used. In the present study, along with the X-band ESR, we applied L-band ESR spectrometry first, which allows for the ESR measurements of Cu(II) complexes under lower dielectric loss by water molecules than that of X-band ESR. X- and L-band ESR parameters analyzed for Cu(II) complexes with CuN_4 coordination mode were found to relate to the coordination structures of the Cu(II) complexes and to other physical parameters, such as stability constants and halfwave potentials of the complexes. Several important features were observed in both the X- and L-band ESR spectra of the Cu(II) complexes as follows: Coordination to the axial positions or tetrahedral distortion of the square-planar Cu(II) complexes decreased in the hyperfine coupling constant, A-value. The g-value decreased when the stability constants increase or when the halfwave potentials shift to become more negative. Both X- and L-band ESR spectrometries are proposed to be very useful for analyzing the coordination structures of Cu(II) complexes in aqueous solutions.

Key words X-band ESR; L-band ESR; copper(II) complex; coordination structure; hyperfine coupling constant; g-value

The functions of the copper ion in copper proteins or enzymes have become clear, and the coordination structures of copper, which center in proteins or enzymes, have been recognized to relate deeply to their functions.[2] Thus, it is important to investigate the coordination structure of the proteins or enzymes. To determine the structures of copper complexes involving copper proteins and enzymes, an X-ray diffraction method has been mainly used.[2b] However, the preparation of a good single crystal available for the method is often very hard. On the other hand, the X-band ESR method has been proven to be useful to know the electronic state around copper(II) ion with a lone-pair electron.[3] Thus, X-band ESR spectroscopy is an important method for investigating the coordination structures of copper(II) complexes in aqueous solutions.[3,4] By plotting ESR parameters such as $g_{/\!/}$-values and hyperfine coupling constant $A_{/\!/}$-values, useful information for the structural analysis of copper(II) complexes are obtained. For example, Peisach and Blumberg reported that a decrease in the charge of the copper(II) complex decreases the complex in $g_{/\!/}$-value but increases the $A_{/\!/}$-value for the complex with the same coordination mode.[5] Further, Yokoi and Addison proposed that the $g_{/\!/}$-value increases but the $A_{/\!/}$-value decreases as the coordination structure of the copper(II) complex changes from a square planar to a tetrahedrally distorted structure depending on the bulkiness of the substituent on the ligand.[6] These reports indicate that X-band ESR parameters are strongly related to the coordination structure of copper(II) complexes. Furthermore, several studies found the occurrence of a relationship between ESR parameters and other physical properties, such as the pK_a-value of the ligand and the redox potential of the copper(II) complex.[6,7]

Although the X-band ESR method is useful for investigating the structures of paramagnetic metal complexes, it is generally hard to detect paramagnetic metal ions in aqueous solutions at room temperature, since X-band microwave (around 9 GHz) is absorbed by a water molecule which has a high dielectric constant. On the other hand, L-band microwave (around 1 GHz) has little dielectric loss by water.[8] Therefore, the L-band ESR method is expected to be useful for measuring paramagnetic metal ions in an aqueous solution or in biological samples with high water contents at room temperature. However, since an L-band ESR spectrometer is less sensitive than an X-band ESR spectrometer, paramagnetic metal ions in aqueous solutions or in biological systems have not been measured after using an L-band ESR spectrometer.[9,10] Thus, a fundamental study on measuring paramagnetic ions in aqueous solutions using an L-band ESR spectrometer is highly needed.

Recently, we found that ESR parameters such as g- and A-values depend on the coordination structure, stability constant and redox potential of five-membered copper(II) complexes of ethylenediamine and its related ligands.[11] In the present study, we extended our work on 5- and 6-membered copper(II) complexes with a CuN_4 coordination mode by both X- and L-band ESR methods in terms of the relationship between ESR parameters and the coordination structures.

Experimental

Materials Copper(II) sulfate ($Cu(II)SO_4 \cdot 5H_2O$) and tetra-*n*-butylammonium perchlorate were purchased from Nacalai Tesque (Japan). tn, N-Me-tn, N,N-Me_2-tn, Me_4-tn, N,N-Et_2-tn, 2,2-Me_2-tn, 1-Et-tn, dpt and Me-dpt were obtained from Tokyo Chemical Industry (Japan). N-Pr-tn and Me_4-dpt were from Aldrich Chemical (Germany). All ligands used are listed in Table 1.

Methods Cu(II) complexes were prepared by mixing a ligand and $CuSO_4$ at various molar ratios in aqueous solutions at various pH values.

X-band ESR spectra were recorded using a JEOL JES RE-3X ESR spectrometer (Japan) at room temperature (22 °C) and at liquid nitrogen temperature (77 K). Instrumental conditions for the ESR measurements were as follows : Modulation frequency 100 kHz, modulation amplitude 0.63 mT and microwave power 5 mW. The magnetic field was calibrated by the splitting of Mn(II) in MgO ($\Delta H_{3-4} = 8.69$ mT), and g-values were standardized with lithium tetracyano-quinodimethane (Li-TCNQ,

---

* To whom correspondence should be addressed.

$g = 2.00252$) as a reference. The concentration of Cu(II) was 5×10^{-4} M at the molar ratio of Cu : ligand = 1 : 0.5—1 : 8. The pH-value was adjusted to 7.4 with 0.1 M NaOH and 0.1 M HCl aqueous solutions. Simulation of the ESR spectra was performed with a JEOL ESPRIT ESR Data System.

L-band ESR spectra were recorded at 22 °C and 77 K with a JEOL JES RE-3L ESR spectrometer equipped with a loop-gap resonator. The Duwar vessel for L-band ESR measurements at 77 K was specially prepared in our laboratory. Instrumental conditions for the ESR measurements were as follows: Modulation frequency 100 kHz, modulation amplitude 1 mT as indicated on the pannel of the spectrometer, and microwave power 15.5 mW. The g-values were calibrated with Li-TCNQ. The concentration of the Cu(II) was 0.1 M at the molar ratio of Cu : ligand = 1 : 1—1 : 8, and the pH-value was adjusted to 10.0 with 0.1 M NaOH and 0.1 M HCl aqueous solutions, since the Cu(II) complexes were precipitated at pH 7.4 due to the use of high concentrations for the L-band ESR measurements.

Simulation of an L-band ESR spectra was performed with an anisotropic simulation program of a JEOL ESPRIT ESR Data System, based on the method of Hurd *et al.*[12] Briefly, L-band ESR spectra were simulated with both ESR parameters (g- and A-values) of the observed L- and X-band spectra by transforming the observed microwave frequency (around 9 GHz) at the X-band ESR to that (1 GHz) at the L-band ESR.

The parallel components, $g_{/\!/}$ and $A_{/\!/}$, were determined from the spectrum at low temperature. The average values, g_0 and A_0, were determined from the ESR spectrum for a Cu(II) complex in free tumbling motions at room temperature. The perpendicular components, $g_{\perp}$ and $A_{\perp}$, were thus calculated by the following relationships,

$$g_0 = (g_{/\!/} + 2g_{\perp})/3$$

and

$$A_0 = (A_{/\!/} + 2A_{\perp})/3$$

The α^2-values for Cu(II) complexes were calculated from the parameters for X-band ESR spectra by the following equation of Kivelson and Neilman,[13]

$$\alpha^2 = A_{/\!/}/P + (g_{/\!/} - 2.0023) + 3/7(g_{\perp} - 2.0023) + 0.04$$
$$P = 360 \times 10^{-4}\,\mathrm{cm}^{-1}$$

Visible absorption spectra were measured at room temperature with a JASCO U-best 55 UV-VIS spectrophotometer (Japan) using quartz cells. The concentration of Cu(II) was 1×10^{-2} M at the molar ratio of Cu : ligand = 1 : 4, and pH values (5—10) were adjusted with 0.1 M NaOH and 0.1 M HCl aqueous solutions.

Cyclic voltammograms were obtained for a solution of acetonitrile–water (acetonitrile : water = 1 : 1) containing 0.1 M tetra-n-butylammonium perchlorate with an electrochemical workstation, BAS 100B/W (U.S.A.). The concentration of Cu(II) was 1×10^{-3} M at the molar ratio of Cu : ligand = 1 : 2. Cyclic voltammetry was performed with a three-electrode system consisting of a glassy-carbon working electrode, a platinum counter electrode and an Ag/AgCl (saturated NaCl) reference electrode. Cyclic voltammograms were recorded at a scan rate of $100\,\mathrm{mVs}^{-1}$. The halfwave potential, $E_{1/2}$, was determined as the midpoint between the peak potentials, E_{pc} and E_{pa}, by the following equation, $E_{1/2} = (E_{\mathrm{pc}} + E_{\mathrm{pa}})/2$. The redox potential E^0 (NHE) was calculated as follows,

$$E^0(\mathrm{NHE}) = E_{1/2}(\mathrm{Ag/AgCl}) + 212\,(\mathrm{mV})$$

The overall stability constants ($\log K_\beta$, $K_\beta = [\mathrm{ML_n}]/[\mathrm{M}][\mathrm{L}]_\mathrm{n}$) of Cu(II)–(N-Me-tn)$_2$ and Cu(II)–(1-Et-tn)$_2$ complexes were determined by potentiometric titration.[14] The titrations were carried out under N_2 in aqueous solutions at the ionic strength $I = 0.1$ (KCl) at 25 °C using a Radiometer TIM90 Titration Manager, ABU91 Autoburette and GK2401C combined glass electrode. The pK_a of the ligand was determined by titrating 2×10^{-3} M ligand aqueous solutions with 0.1 M KOH. The pKa value was calculated using the method described by Albert and Serjent.[14] The $\log K_\beta$ of the complex was determined by titrating a mixture of 2×10^{-3} M ligand and 1×10^{-3} M Cu(II) solution with 0.1 M KOH, and was calculated by using $\bar{n}$ and [L] values, as described by Irving and Rossotti.[15]

Results

X- and L-Band ESR Spectra ESR spectra were obtained at both room (22 °C) and liquid nitrogen (77 K) temperatures. At the molar ratios of Cu : ligand = 1 : 0.5 and 1 : 1, X-band ESR spectra were a little complicated, probably due to the formation of complexes composed of 1 : 1 and 1 : 2 of Cu(II) to ligand. When the molar ratio of the ligand to Cu(II) ion increased, distinct spectra due to the formation of a complex composed of 1 : 2 of Cu(II) to ligand were obtained. However, when dpt, Me-dpt or Me$_4$-dpt was used as a ligand, the spectrum remained almost unchanged due to the formation of a complex composed of 1 : 1 Cu(II) to ligand. On the other hand, L-band ESR spectra were almost unaltered by variations of the molar ratio of Cu : ligand in all systems investigated, because L-band ESR spectra gave rather broader lines than those of the X-band ESR spectra. Figure 1 shows typical spectra for a Cu(II)–(tn)$_2$ complex together with the simulated spectra. The observed spectra in both the X- and L-band ESR measurements were in good agreement with the simulated spectra.

ESR parameters of the Cu(II) complexes thus obtained are summarized in Table 1, in which the indicated configurations of the complexes are those estimated by the reported results of X-ray crystal analyses.[16—33]

Visible Absorption Spectra The visible absorption maxima of the complexes at pH 7.4 are summarized in Table 1. Most complexes examined gave an absorption peak at 550—700 nm and $\varepsilon < 130\,\mathrm{M}^{-1}\,\mathrm{cm}^{-1}$. When the structure of the Cu(II) complexes changes from square-planar to octahedral (axially-coordinate square-planar), tetrahedral or square-pyramidal (Cu ion displaced from the N_4 plane), red shifts of the absorption maximum due to a *d–d* transition were observed,[6,34,35] as reported by the results on Cu(II)–N-alkylsalicylaldiminate complexes.[36]

Halfwave Potentials Figure 2 shows a typical cyclic voltammogram measured for the Cu(II)/Cu(I) coupled reaction in the Cu(II)–(tn)$_2$ complex. The cyclic voltammogram displayed a typical quasi-reversible redox-reaction at $E_{1/2}$ (*vs.* Ag/AgCl electrode). Table 2 summarizes the electrochemical data for the Cu(II) complexes examined.

Stability Constants of the Complex Stability constants unreported in the literature were measured by the potentiometric titration method. The pK_a values of the ligands and $\log K_\beta$ values of the complexes were calculated using the observed titration curves. The pK_a values of the ligands were calculated as follows: p$K_1 = 8.78$ and p$K_2 = 10.59$ for N-Me-tn, and p$K_1 = 8.83$ and p$K_2 = 10.42$ for 1-Et-tn. The $\log K_\beta$ of the complexes are listed in Table 1.

Discussion

Comparison of X- and L-Band ESR Spectra Both X- and L-band ESR spectra were obtained for complexes with a CuN$_4$ coordination mode at both room and liquid nitrogen temperatures. Observed and simulated spectra of the Cu(II)–(en)$_2$ complex are shown in Fig. 1. Although the L-band ESR spectra were found to be broader than those of the X-band ESR spectra, simulation of the L-band

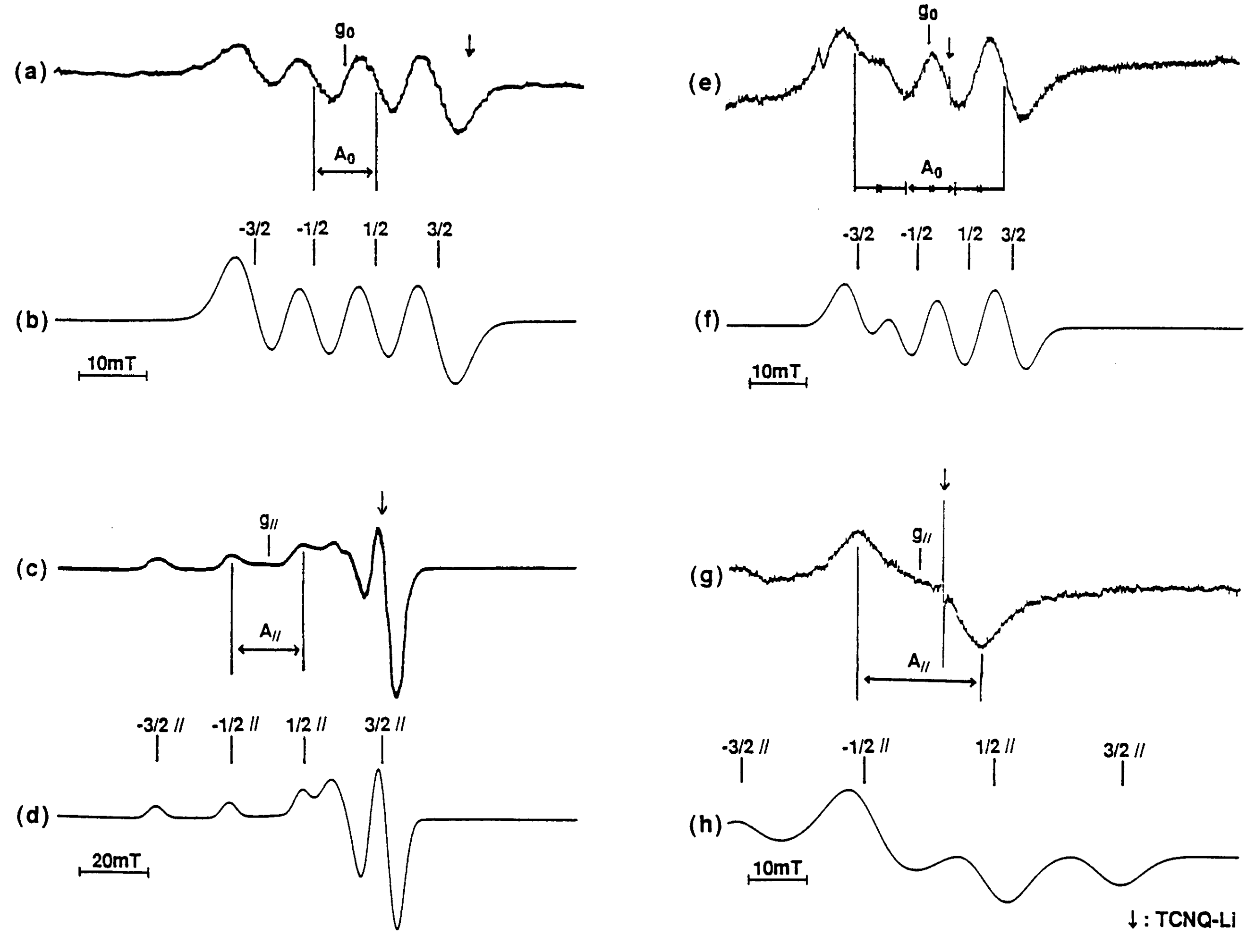

Fig. 1. X- and L-Band ESR Spectra for the Copper(II) Complex of tn in Aqueous Solution

(a) observed X-band ESR spectra at room temperature, (b) simulated X-band ESR spectra at room temperature, (c) observed X-band ESR spectra at liquid nitrogen temperature, (d) simulated X-band ESR spectra at liquid nitrogen temperature, (e) observed L-band ESR spectra at room temperature, (f) simulated L-band ESR spectra at room temperature, (g) observed L-band ESR spectra at liquid nitrogen temperature, (h) simulated L-band ESR spectra at liquid nitrogen temperature. (a) and (c): The complex was prepared at the molar ratio of Cu(II) : ligand = 1 : 4 (Cu(II) = 0.5 mM) at pH 7.4. (e) and (g): The complex was prepared at the molar ratio of Cu(II) : ligand = 1 : 4 (Cu(II) = 100 mM) at pH 10.0.

ESR spectra could be performed by using both the X-band ESR parameters (g- and A-values) and the microwave frequency transformed from the X-band (around 9 GHz) to the L-band (1 GHz). The simulated spectra were found to be almost identical to the observed spectra, as shown in Fig. 1, indicating that the parameters of the L-band ESR spectra are essentially identical to those of X-band ESR spectra. Further theoretical investigation of the analysis of L-band ESR spectra will be needed in the future.

Relationship between ESR Parameters and Stability Constants or Halfwave Potentials for Cu(II) Complexes Cu(II) complexes with various coordination structures, such as square-planar, octahedral, tetrahedral or square-pyramidal configurations, were examined in terms of the ESR parameters. Each configuration of the Cu(II) complexes was estimated by the certified X-ray crystallographic analyses reported before.[16—33]

Figure 3 shows a plot of $A_{/\!/}$ against $g_{/\!/}$ for all Cu(II) complexes examined. Square-planar complexes in the CuN_4 mode (No. 1—15), as indicated by the A-field in Fig. 3, have relatively large $A_{/\!/}$-values compared with those for the complexes in other coordination modes (B-, C-, D-fields). Cu(II) complexes of tn and its related ligands (No. 1—7) form two six-membered ring chelates. On the other hand, Cu(II)–(en)$_2$ and its related complexes (No. 8—15) form two five-membered ring chelates. In general, the stability constants ($\log K_\beta = 16.4$ on average in Table 1) of six-membered ring chelates are lower than those ($\log K_\beta = 17.3$ on average in Table 1) of the corresponding five-membered ring chelates.[37,38] The complexes of the six-membered chelates appear to have relatively large $g_{/\!/}$-values (2.232 in average) and small $A_{/\!/}$-values ($194.1 \times 10^{-4}\,\mathrm{cm}^{-1}$ in average) compared with those (2.217 and $198.4 \times 10^{-4}\,\mathrm{cm}^{-1}$ on average) of the five-membered chelate. Cu(II) complexes with CuN_3 type coordination (No. 16—18, B-field in Fig. 3) gave smaller $A_{/\!/}$-values and larger $g_{/\!/}$-values than those in the CuN_4 mode, and were distributed in a different region in the plotting. Further, octahedral (No. 19—21, C-field in Fig. 3) and tetrahedral complexes (No. 22—24, D-field in Fig. 3) have relatively small $A_{/\!/}$-values. Thus, those complexes are distributed in different regions from each other in the plotting. Similarly, a plot of A_0 against g_0 was also found to depend on the coordination structure of Cu(II) complexes (Fig. 4). In octahedral or tetrahedral complexes, coordination to the axial position or tetrahedral distortion

Table 1. X-Band ESR Parameters for the Cu(II) Complexes

Complex No.	Ligand	g-value			A-value (10^{-4} cm^{-1})			α^2	log K_β[b]	λ_{max}	ε
		g_0	$g_{/\!/}$	$g_\perp$	A_0	$A_{/\!/}$	$A_\perp$			(nm)	(M^{-1}cm^{-1})
	Square-planar (N$_4$ coordination mode)										
1	(tn)$_2$	2.109	2.220	2.053	78.6	202.6	21.1	0.84	17.0	568	106
2	(N-Me-tn)$_2$	2.123	2.248	2.060	74.0	184.1	23.3	0.82	13.1[c]	632	110
3	(N,N-Me$_2$-tn)$_2$	2.123	2.251	2.059	70.5	183.2	18.7	0.82	—[d]	631	138
4	(N,N-Et$_2$-tn)$_2$	2.123	2.246	2.061	74.5	191.8	20.5	0.84	—[d]	630	112
5	(N-Pr-tn)$_2$	2.122	2.232	2.067	73.2	199.7	14.5	0.85	—[d]	633	130
6	(2,2-Me$_2$-tn)$_2$	2.108	2.213	2.056	82.3	200.1	27.4	0.83	17.4	560	116
7	(1-Et-tn)$_2$	2.109	2.215	2.057	81.3	197.0	27.4	0.82	17.9[c]	565	126
	(Average)		2.232			194.1			16.4		
8	(en)$_2$[a]	2.101	2.204	2.050	82.9	209.5	23.8	0.84	19.6	547	128
9	(N-Me-en)$_2$[a]	2.104	2.208	2.052	83.2	203.2	27.3	0.83	18.9	551	84
10	(N,N-Me$_2$-en)$_2$[a]	2.104	2.203	2.055	80.3	200.0	24.4	0.82	16.4	564	156
11	(N,N′-Me$_2$-en)$_2$[a]	2.106	2.214	2.052	82.8	200.3	28.2	0.83	17.1	565	107
12	(N-Et-en)$_2$[a]	2.104	2.208	2.052	82.4	202.1	26.7	0.83	18.6	558	112
13	(N,N-Et$_2$-en)$_2$[a]	2.114	2.247	2.048	79.7	186.3	30.8	0.82	13.7	585	210
14	(N,N′-Et$_2$-en)$_2$[a]	2.118	2.248	2.053	74.5	185.8	23.5	0.82	15.6	583	108
15	(N-Pr-en)$_2$[a]	2.104	2.207	2.053	82.2	200.3	27.1	0.82	18.1	559	104
	(Average)		2.217			198.4			17.3		
	N$_3$ coordination mode										
16	dpt	2.118	2.241	2.056	76.0	174.0	30.8	0.79	14.2	611	112
17	Me-dpt	2.121	2.241	2.060	70.9	180.2	20.6	0.80	12.5	627	132
18	Me$_4$-dpt	2.127	2.261	2.060	70.3	173.2	23.3	0.80	—[d]	673	74
	Octahedral										
19	(dien)$_2$[a]	2.113	2.212	2.064	65.4	181.7	11.1	0.78	20.9	630	110
20	tetren[a]	2.110	2.205	2.063	66.7	163.2	21.4	0.72	22.8	645	166
21	hexen[a]	2.110	2.203	2.064	66.7	167.6	19.3	0.73	22.1	627	236
	Tetrahedral										
22.	(bipy)$_2$[a]	2.145	2.259	2.088	59.5	156.1	14.7	0.77	12.7	700	72
23.	(phen)$_2$[a]	2.145	2.271	2.082	57.3	155.8	12.0	0.78	11.1	690	42
24.	(Me$_4$-tn)$_2$	2.125	2.257	2.059	70.81	176.3	22.5	0.81	—[d]	654	138
	Square-pyramidal										
25.	trien[a]	2.102	2.200	2.053	80.8	200.2	24.9	0.82	20.1	587	144
26.	cyclen[a]	2.103	2.200	2.054	76.0	191.3	22.1	0.79	24.8	605	202

[a] Sawada T., Fukumaru K., Sakurai H., *Chem. Pharm. Bull.*, **44**, 1009—1016 (1996). [b] Martell A. E., Critical Stability Constants, vol. 2 Amines, vol. 5 First Supplement (1982). [c] Measured by potentiometric titration. [d] Data were not calculated due to the formation of precipitation during the titration under the same aqueous conditions.

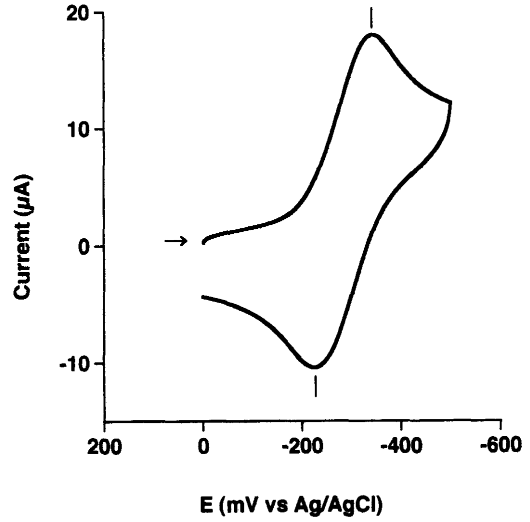

Fig. 2. Cyclic Voltammogram for a Copper(II) Complex of tn in Acetonitrile–Water (1:1) Containing 0.1 M tetra-*n*-Butyl Ammonium Perchlorate

The complex was prepared at a molar ratio of Cu(II):ligand = 1:2 (Cu(II) = 1 mM) in 50% acetonitrile solution. Numbers for the complex refer to those in Table 1.

Table 2. Electrochemical Data for the Cu(II) Complexes

Ligand	E_{pc} (mV)	E_{pa} (mV)	$E_{1/2}$ (mV)
(tn)$_2$	−338	−241	−290
(N-Me-tn)$_2$	−187	−51	−119
(N,N-Me$_2$-tn)$_2$	−71	32	−20
(N-Pr-tn)$_2$	−136	−12	−74
(2,2-Me$_2$-tn)$_2$	−349	−248	−299
(1-Et-tn)$_2$	−339	−238	−289
(en)$_2$	−472	−353	−413
(N-Me-en)$_2$	−445	−310	−378
(N,N-Me$_2$-en)$_2$	−257	−145	−201
(N,N′-Me$_2$-en)$_2$	−332	−188	−260
(N-Et-en)$_2$	−332	−222	−277
(N,N-Et$_2$-en)$_2$	−97	12	−43
(N,N′-Et$_2$-en)$_2$	−131	−20	−76
(N-Pr-en)$_2$	−302	−196	−249
dpt	−317	−12	−74
Me-dpt	−201	−107	−154
(dien)$_2$	−509	−409	−459
tetren	−697	−617	−657
hexen	−662	−571	−617
(bipy)$_2$	33	127	80
(phen)$_2$	6	103	55
trien	−561	−473	−517
cyclen	−646	−588	−617

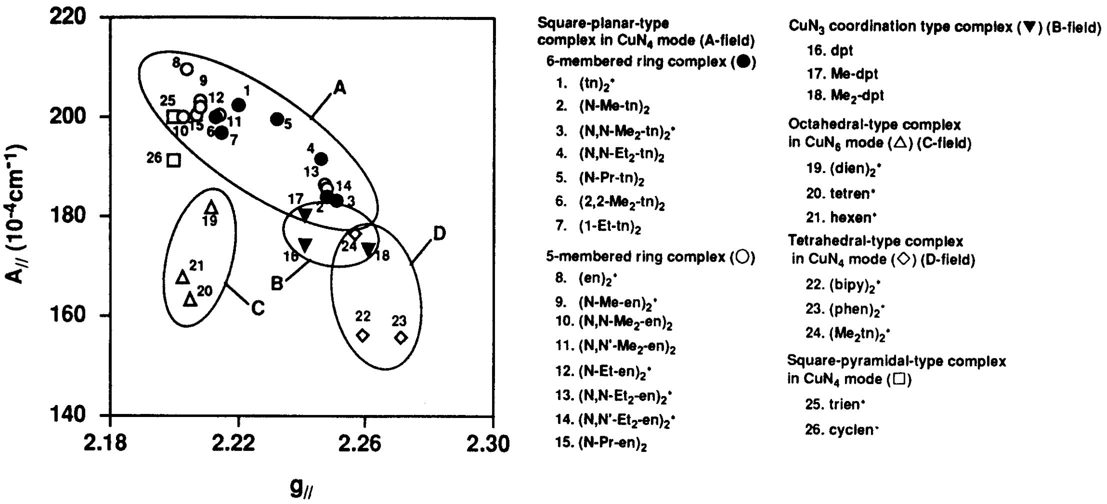

Fig. 3. Relationship between $g_{//}$-Values and $A_{//}$-Values for the Copper(II) Complex

* The structure of the complex was analyzed by X-ray crystallography.[16–33] Numbers for the complex refer to those in Table 1.

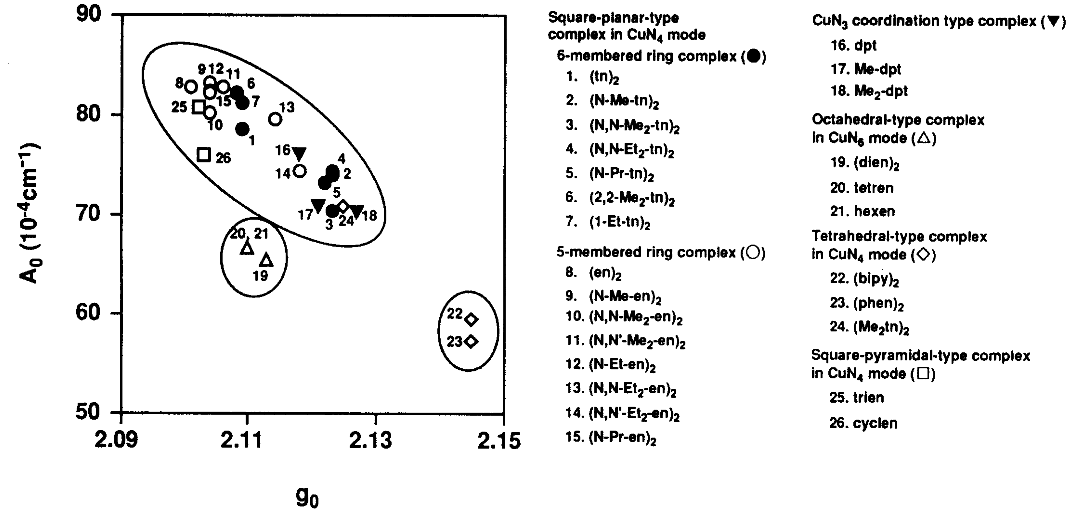

Fig. 4. Relationship between g_0-Values and A_0-Values for the Copper(II) Complex

* The structure of the complex was analyzed by X-ray crystallography.[16–33] Numbers for the complex refer to those in Table 1.

has been reported to weaken the coordination bond in a plane of the complex, which results in a decrease in the $A_{//}$-value.[6] Thus, a Cu(II) complex with a high electron density is estimated to have a large A-value and a small g-value, suggesting that distribution in a different region in the plotting of ESR parameters is based on the difference in electron density on the Cu(II) ion. In addition, we calculated the α^2-value (Table 1), which evaluates an unpaired electron density on the d-orbital of the Cu(II) ion as proposed by Kivelson and Neilman.[13] Square-planar complexes which gave large A-values showed relatively large α^2-values, while octahedral and tetrahedral complexes which gave small A-values showed small α^2-values. Based on these results, we conclude that the coordination structure of the Cu(II) complex can be estimated by plotting ESR parameters such as A and g-values.

Furthermore, we investigated the relationship between ESR parameters and other physical properties, such as the overall stability constant ($\log K_\beta$) or halfwave potential of the complex. When $\log K_\beta$-values were plotted against the $g_{//}$-values of the complexes involving all coordination modes, a good linear relationship was found, with a correlation coefficient of $r=0.867$ of the linear regression for a total of 21 points, as shown in Fig. 5. In addition, a good relationship between $\log K_\beta$ and $A_{//}$-values was observed for the square-planar complexes, as shown in Fig. 5 (correlation coefficient $r=0.906$ for a total of 12 points). Similarly, g_0 or A_0 was plotted against $\log K_\beta$, and almost the same tendencies were observed as the plot of $g_{//}$ or $A_{//}$ against $\log K_\beta$ (data not shown), where in other coordination complexes, except the square-planar complexes, linear relationships were not found.

The pK_a-values of ligands in Cu(II) complexes have been reported to relate linearly to the $g_{//}$-values in Cu(II)-β-diketone complexes.[7] However, no relationship between the stability constants of the Cu(II) complexes and ESR parameters (g- and A-values) has been proposed so far. The stability constant of the complex is considered to relate to the electron donating ability, from a ligand to a metal ion. A complex which has a high stability constant possesses a high electron density at the Cu(II) site.

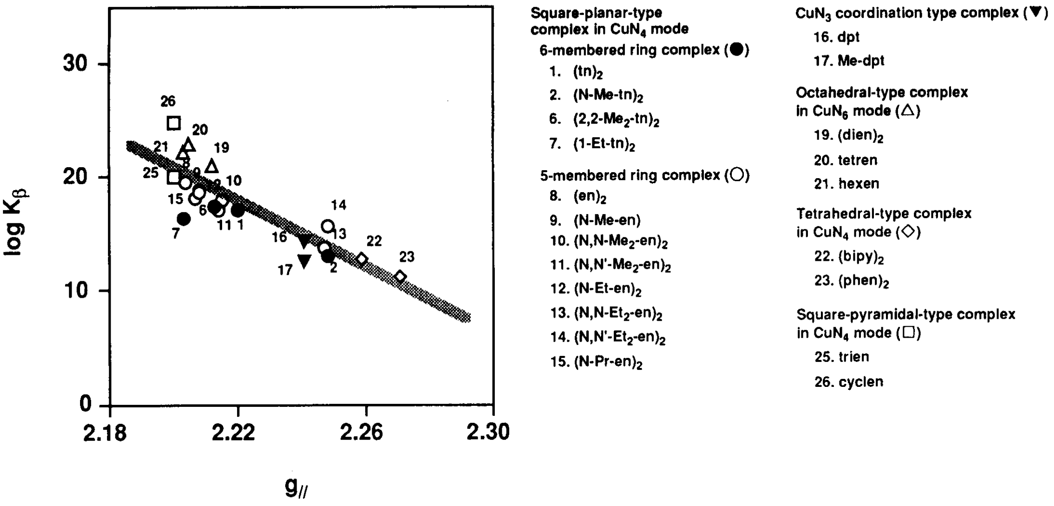

Fig. 5. Relationship between $g_{//}$-Value and $\log K_\beta$ for the Copper(II) Complexes

The correlation coefficient of the linear regression was $r=0.867$ for a total of 21 points. Numbers for the complex refer to those in Table 1.

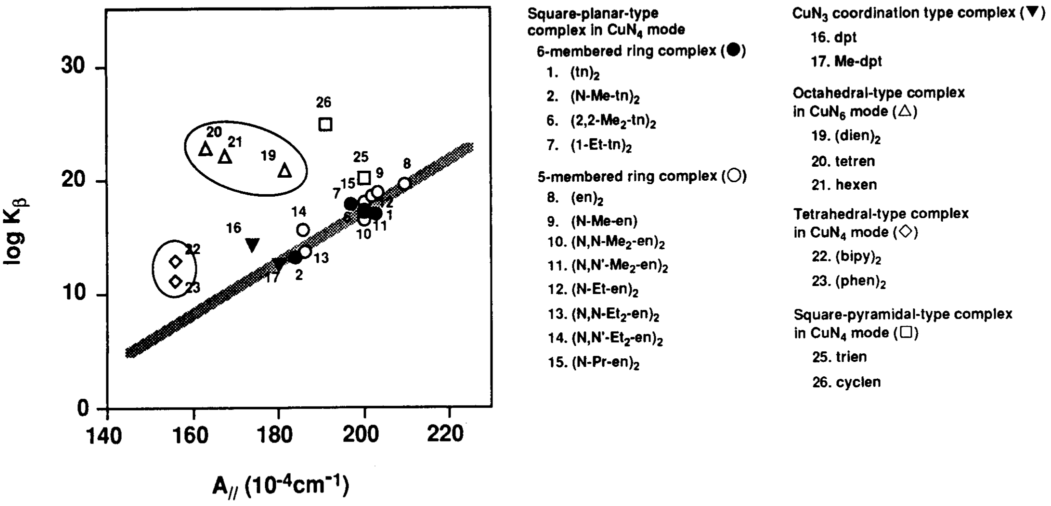

Fig. 6. Relationship between $\log K_\beta$ and $A_{//}$-Value for the Copper(II) Complex

The correlation coefficient of the linear regression was $r=0.906$ for a total of 12 points. Numbers for the complex refer to those in Table 1.

Consequently, it was observed that as the complex has a high stability constant, the *A*-value increases and the *g*-value decreases. Comparison of Figs. 5 and 6 indicates that the *A*-value is affected by a change in the coordination structure of the complex. The *A*-value is indicated to be closely related to the strength of the coordinate bond in a planar model of the complex and in a distortion of the planar.

The electron density of the Cu(II) complex depends on the redox potential of the complex. Therefore, we investigated the relationship between the redox potential and ESR parameter of the Cu(II) complex. The redox potential of the Cu(II)/Cu(I) couple has been known to shift to a more positive value by the destabilization of the Cu(II) species, due to steric hindrance of a ligand or tetrahedral distorted structure.[6),7)] In fact, we obtained the result that Cu(II) complexes of N-alkyl-propanediamines have relatively more positive halfwave potentials than that of Cu(II)–(tn)$_2$, owing to destabilization by the steric hindrance of alkyl substituents (Table 2). Cu(II)–(tn)$_2$, –(Me-tn)$_2$ and –(Me$_2$-tn)$_2$ complexes gave more positive halfwave potentials than those of Cu(II)–(en)$_2$, –(Me-en)$_2$ and –(Me$_2$-en)$_2$, respectively. These results suggest that the complexes of the six-membered ring chelate are less stable than the corresponding complexes of the five-membered ring chelate. The plot of halfwave potential ($E_{1/2}$) against $\log K_\beta$ gave a good linear relationship (Fig. 7). In addition, linear relationships for the $g_{//}$-value and halfwave potential was also obtained, the correlation coefficient being $r=0.847$ of the linear regression for a total of 23 points, as shown in Fig. 8. On the basis of the results, we conclude that the ESR parameters, overall stability constant and halfwave potential of the Cu(II) complexes relate to each other in terms of electron density on Cu(II) center. However, no linear relationship for the $A_{//}$-value and halfwave potential ($E_{1/2}$) was observed, probably due to the presence of many factors contributing to the *A*-values, such as the steric configuration of the complexes, distribution of several complex forms at an equilibrium state, and the strength of the coordination bonds.

Comparison of L-Band ESR Spectra with X-Band ESR Spectra X-band ESR parameters have been concluded to reflect on the coordination structure of the Cu(II)

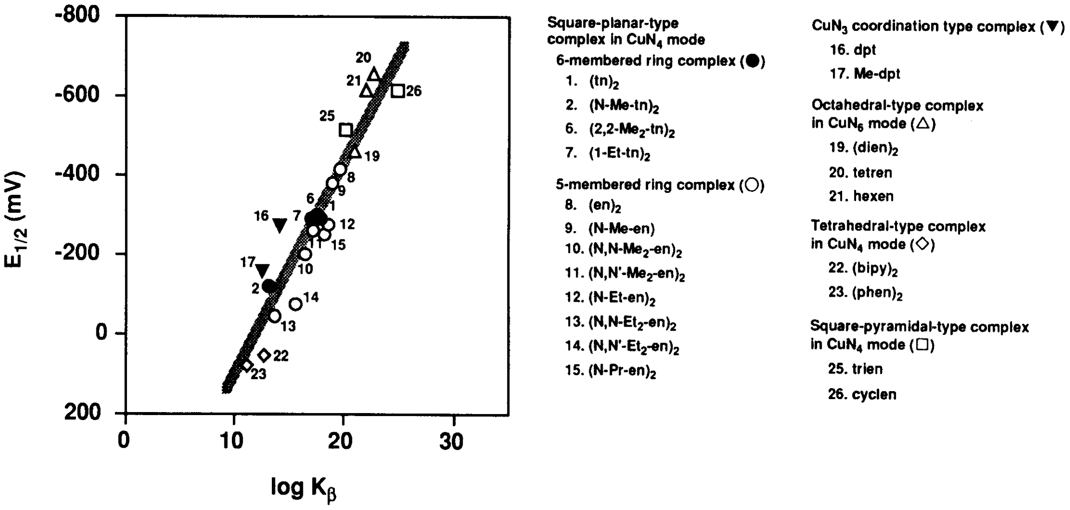

Fig. 7. Relationships between $E_{1/2}$ and $\log K_\beta$ for the Copper(II) Complexes

The correlation coefficient of the linear regression was $r=0.937$ for a total of 21 points. Numbers for the complex refer to those in Table 1.

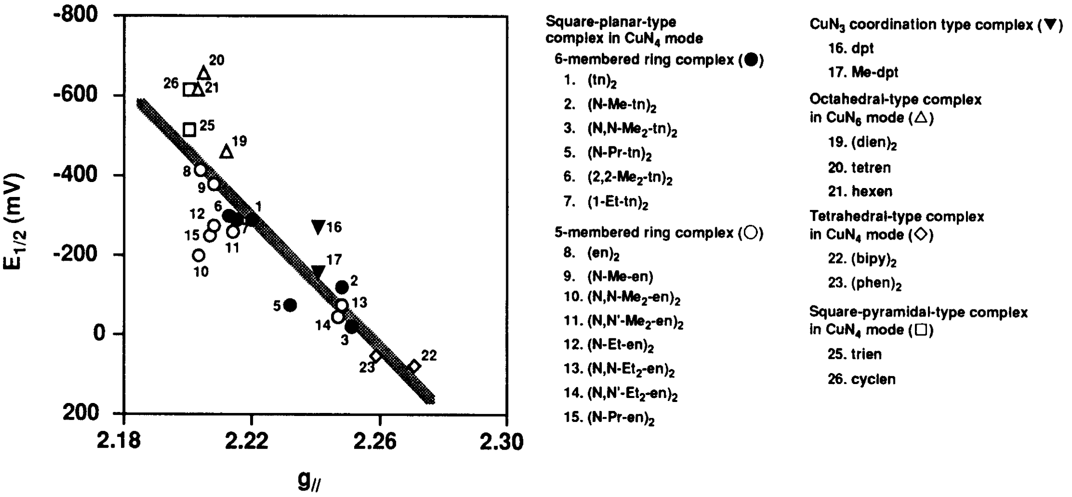

Fig. 8. Relationships between $g_{//}$-Value and $E_{1/2}$ for the Copper(II) Complexes

The correlation coefficient of the linear regression was $r=0.847$ for a total of 23 points. Numbers for the complex refer to those in Table 1.

Table 3. L-Band ESR Parameters for the Cu(II) Complexes

Ligand	${}^{L}g$-value			${}^{L}A$-value (10^{-4} cm^{-1})		
	${}^{L}g_0$	${}^{L}g_{//}$	${}^{L}g_{\perp}$	${}^{L}A_0$	${}^{L}A_{//}$	${}^{L}A_{\perp}$
Square-planar (N_4 coordination mode)						
$(tn)_2$	2.159	2.233	2.122	81.8	212.7	16.4
$(N\text{-}Me\text{-}tn)_2$	2.159	2.243	2.117	77.3	207.7	12.1
$(N\text{-}Pr\text{-}tn)_2$	2.192	2.229	2.174	81.0	209.2	16.9
$(2,2\text{-}Me_2\text{-}tn)_2$	2.201	2.232	2.186	87.7	215.4	23.9
$(1\text{-}Et\text{-}tn)_2$	2.191	2.233	2.170	86.5	209.2	25.2
$(en)_2$	2.156	2.231	2.119	88.2	217.4	23.6
$(N\text{-}Me\text{-}en)_2$	2.187	2.238	2.162	89.3	219.1	24.4
$(N,N\text{-}Me_2\text{-}en)_2$	2.187	2.228	2.167	84.8	212.2	21.1
$(N,N'\text{-}Me_2\text{-}en)_2$	2.191	2.238	2.168	87.0	212.1	24.5
$(N\text{-}Et\text{-}en)_2$	2.195	2.230	2.178	89.2	213.8	26.9
$(N,N\text{-}Et_2\text{-}en)_2$	2.178	2.233	2.151	77.1	198.1	16.6
$(N,N'\text{-}Et_2\text{-}en)_2$	2.214	2.234	2.204	87.3	210.7	25.6
$(N\text{-}Pr\text{-}en)_2$	2.196	2.235	2.177	88.5	216.7	24.4
N_3 coordination mode						
dpt	2.172	2.256	2.130	77.0	206.8	12.1
Me-dpt	2.162	2.234	2.126	72.6	202.0	7.9
Octahedral						
$(dien)_2$	2.157	2.244	2.114	66.9	203.9	—
tetren	2.156	2.250	2.109	67.1	202.7	—
hexen	2.162	2.249	2.119	68.4	199.2	3.0
Square-pyramidal						
trien	2.182	2.259	2.144	86.1	206.3	26.0
cyclen	2.142	2.209	2.109	78.1	193.9	20.2

complex. Thus, we studied the relationship of the coordination structure of the complex and L-band ESR parameters (${}^{L}g_0$, ${}^{L}A_0$) (Table 3). Figure 9 shows a plot of ${}^{L}A_0$ against ${}^{L}g_0$ for the complexes. As described above, the A_0–g_0 plot of X-band ESR parameters obtained at room temperature for the Cu(II) complexes indicated a clear distribution depending on the coordination mode, as shown in Fig. 4. However, the ${}^{L}A_0$–${}^{L}g_0$ plot for the

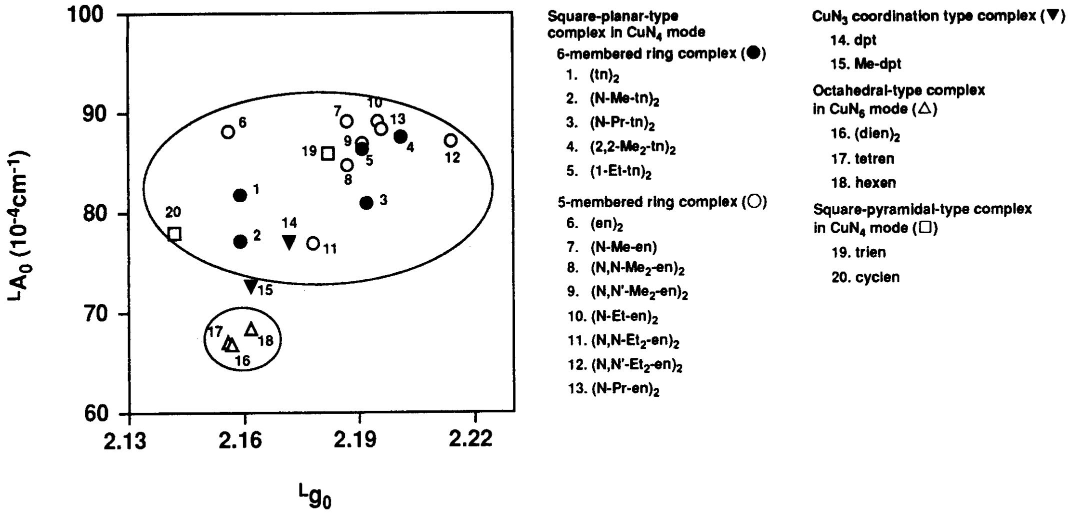

Fig. 9. Relationship between $^{L}g_0$-Values and $^{L}A_0$-Values for the Copper(II) Complex

Numbers for the complex refer to those in Table 1.

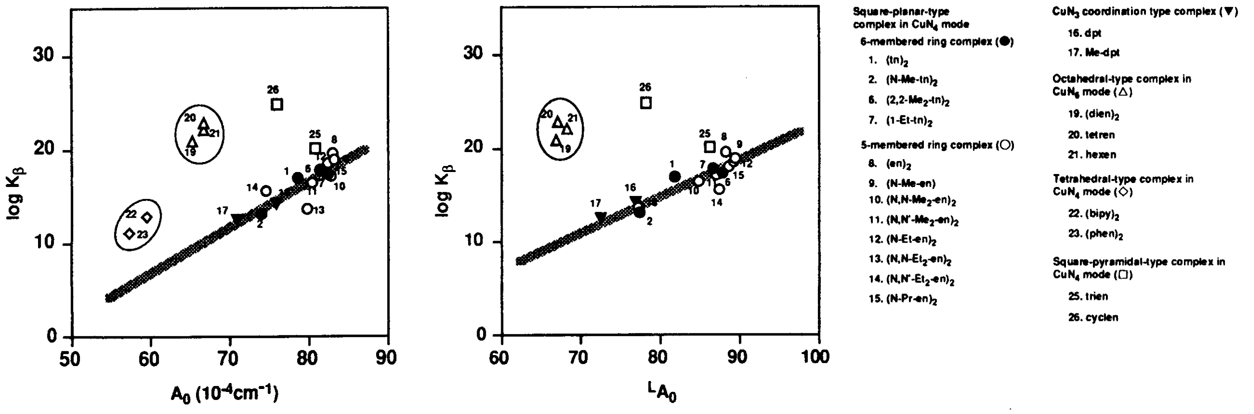

Fig. 10. Relationship between the A_0-Values and $\log K_\beta$ and between the $^{L}A_0$-Values and $\log K_\beta$ for the Copper(II) Complex

Numbers for the complex refer to those in Table 1. Correlation coefficients of the linear regression were $r=0.782$ for a total of 12 points for the plotted A_0-values, and $r=0.873$ for a total of 12 points for the plotted $^{L}A_0$-values.

same Cu(II) complexes gave an indistinct distribution depending on the coordination mode, except for the octahedral type complexes. In spite of these observations, the axial-coordination or distortion of square-planar models by the steric hindrance of ligands showed a tendency to decrease the $^{L}A_0$-value, but did not give any distinct tendency for the $^{L}g_0$-value. Although the analysis of the $^{L}g_0$-value of the Cu(II) complex needs to be investigated further, the L-band ESR parameters were suggested to reflect the coordination structure of the complex to some degree. Moreover, the relationships between $^{L}g_0$ or $^{L}A_0$ and $\log K_\beta$ were found to be similar to those seen in the X-band ESR parameters. For example, a good relationship between $^{L}A_0$ and $\log K_\beta$ was observed in the square-planar type complexes, similarly to that between A_0 (X-band) and $\log K_\beta$ (Fig. 10). L-band ESR spectrometry is thus considered to be useful for determining the coordination structure of Cu(II) complexes in aqueous solutions. These results might be useful for determining the coordination structure of Cu(II)–proteins or enzymes in aqueous solutions in the future. Further investigations are in progress.

Conclusion

X-band ESR parameters were found to relate significantly to the coordination structure, over all stability constant and halfwave potential of the Cu(II) complexes. L-band ESR parameters showed a similar tendency to those of X-band ESR. Both X- and L-band ESR spectrometries are thus suggested to be very useful for analyzing the coordination structures of Cu(II) complexes in aqueous solutions.

Acknowledgment This work was partially supported by Grant-in-Aids for Scientific Research from the Ministry of Education, Science, Sports and Culture.

References and Notes

1) Abbreviations: tn (1,3-propanediamine), N-Me-tn (*N*-methyl-1,3-propanediamine), N,N-Me$_2$tn (*N,N*-dimethyl-1,3-propanediamine), N,N-Et$_2$-tn (*N,N*-diethyl-1,3-propanediamine), N-Pr-tn (*N*-propyl-1,3-propanediamine), 2,2-Me$_2$-tn (2,2-dimethyl-1,3-propanediamine), 1-Et-tn (1,3-pentanediamine), en (ethylenediamine), N-Me-en (*N*-methylethylenediamine), N,N-Me$_2$-en (*N,N*-dimethylethylenediamine), N,N'-Me$_2$-en (*N,N'*-dimethylethylenediamine), N-Et-en (*N*-ethylethylenediamine), N-Pr-en (*N*-propylethylenediamine), dpt (3,3'-diaminodipropylamine), Me-dpt (*N,N*-bis(3-aminopropyl)-methylamine), Me$_4$-dpt (3,3'-iminobis (*N,N*-dimethylpropylamine)), dien (diethylenetriamine), trien (triethylenetetramine),

tetren (tetraethylenepentamine), hexen (pentaethylenehexamine), bipy (2,2′-bipyridine), phen (1,10-phenanthroline), cyclen (1,4,7,10-tetraazacyclododecane tetrahydrochloride), Li-TCNQ (tetracyano quinodimethane lithium salt), ESR (electron spin resonance), log K_β (over-all stability constant), E_{pa} (oxidation potential), E_{pc} (reduction potential), $E_{1/2}$ (halfwave potential).

2) *a*) Boas J. F., Pilbrow J. R., Smith T. D., *Biological Magnetic Resonance*, **1**, 277—342 (1978); *b*) Ibers J. A., Holm R. H., *Science*, **209**, 223—235 (1980); Kitajima N., *Adv. Inorg. Chem.*, **39**, 1—77 (1992); Solomon E. I., Lowery M. D., *Science*, **259**, 1575—1581 (1993); Karlin K. D., *ibid.*, **261**, 701—708 (1993).

3) Vänngård T., "Biological Applications of Electron Spin Resonance," ed. by Swartz H. M., Bolton J. R., Borg D. C., Wiley-Interscience, New York, 1972, pp. 411—447.

4) Malmström B. G., Mosbach R., Vänngård T., *Nature* (London), **183**, 321—322 (1959).

5) Peisach J., Blumberg W. E., *Arch. Biochem. Biophys.*, **165**, 691—708 (1974).

6) Yokoi H., Addison A. W., *Inorg. Chem.*, **16**, 1341—1349 (1977).

7) James B. R., Williams J. P., *J. Chem. Soc.*, **1961**, 2007—2019.

8) Ray P. S., *Appl. Opt.*, **11**, 1836—1844 (1972).

9) Liu K. J., Tiang J., Swartz H. M., Shi X., *Arch. Biochem. Biophys*, **313**, 248—252 (1994).

10) Utsumi H., Tatebe T., Hamada H., *Chem. Lett.*, **1992**, 277—280.

11) Sawada T., Fukumaru K., Sakurai H., *Chem. Pharm. Bull.*, **44**, 1009—1016 (1996); *idem*, *Biochem. Biophys. Res. Commun.*, **216**, 154—161 (1995).

12) Hurd F. K., Sachs M., Hershberger W. D., *Phys. Rev.*, **93**, 373—380 (1954).

13) Kivelson D., Neilman R., *J. Chem. Phys.*, **35**, 149—155 (1961).

14) Albert A., Serjent E. P., "Ionization Constants of Acids and Bases," Methuen, London, 1962.

15) Irving H., Rossotti H. S., *J. Chem. Soc.*, **1953**, 3397—3405.

16) Pajunen A., *Suom. Kemistil. B*, **42**, 15—18 (1969).

17) Pajunen A., Belinskij I., *Suom. Kemistil. B*, **43**, 70—74 (1970).

18) Uggla R., Klinga M., *Suom. Kemistil. B*, **45**, 10—15 (1972).

19) Bertini I., Mani F., *Inorg. Chem.*, **6**, 2032—2035 (1967).

20) Komiyama Y., Lingafelter E. C., *Acta. Crystallogr.*, **17**, 1145—1148 (1964).

21) Brown B. W., Lingafelter E. C., *Acta. Crystallogr.*, **17**, 254—259 (1964).

22) Emsley J., Arif M., *J. Mol. Struct.*, **220**, 1—12 (1990).

23) Luukkonen E., Pajunen A., *Suom. Kemistil. B*, **42**, 474—477 (1969).

24) Grenthe I., Paoletti P., Sandstöm M., Glikberg S., *Inorg. Chem.*, **18**, 2687—2692 (1979).

25) Pajunen A., Luukkonen E., *Suom. Kemistil. B*, **42**, 348—353 (1969).

26) Hathaway B. J., Bew M. J., Billing D. E., Dudley R. J., Nicholls P., *J. Chem. Soc. A*, **1969**, 2312—2318.

27) Stephens F. S., *J. Chem. Soc. A*, **1969**, 2233—2240.

28) Stephens F. S., *J. Chem. Soc. A*, **1969**, 883—890.

29) Nakai H., *Bull. Chem. Soc. Jpn.*, **56**, 1637—1641 (1983).

30) Amournjarusiri K., Hathaway B. J., *Acta. Crystallogr. Sect. C*, **47**, 1383—1385 (1991).

31) Marongiu G., Lingafelter E. C., Paoletti P., *Inorg. Chem.*, **8**, 2763—2767 (1969).

32) Clay R., Murray-Rust P., Murray-Rust J., *Acta. Crystallogr. Sect. B*, **35**, 1894—1895 (1979).

33) Jonassen H. B., Bertrand J. A., Groves F. R., Jr., Stearns R. I., *J. Am. Chem. Soc.*, **79**, 4279—4282 (1957).

34) Murakami Y., Matsuda Y., Sakata K., *Inorg. Chem.*, **10**, 1728—1734 (1971).

35) Yokoi H., *Bull. Chem. Soc. Jpn.*, **47**, 3037—3040 (1974).

36) Sinn E., Harris C. M., *Coord. Chem. Rev.*, **4**, 391—422 (1969).

37) Bailar J. C., Jr., Work J. B., *J. Am. Chem. Soc.*, **68**, 232—235 (1946).

38) Irving H., Williams R. J. P., Ferrett D. J., Williams A. E., *J. Chem. Soc.*, **1954**, 3494—3504.